LETTER TO THE EDITOR



A nonconformal nonlocal approach to calculating statistical spread in fatigue indicator parameters for polycrystals

John A. Moore¹ | Caitlin Martinez¹ | Ayushi Chandel²

Correspondence

John A. Moore, Department of Mechanical Engineering, Marquette University, Milwaukee, WI, USA. Email: john.a.moore@marquette.edu

Funding information

National Science Foundation, Grant/Award Number: 1934753

This letter presents an extension of the fatigue indicator parameter work in Castelluccio and McDowell.¹

In the study of fatigue fracture in metals, fatigue indicator parameters (FIPs) are nonlocal quantities that represent the driving force to incubate fatigue cracks¹ and correlate well to crack tip opening displacement.² FIP is often related directly to fatigue life N. These FIP values can be used to design materials with microstructural features less prone to fatigue failure. 1,2 However, the nonlocal nature of FIPs introduces another variable that must be determined for accurate predictions. Many studies use nonlocal volumes that enclose a predetermined number of finite elements. To encapsulate the entire microstructure, these nonlocal volumes must be conformal to the microstructure (i.e., they do not overlap or have gaps between them). These nonlocal volumes intrinsically have a length scale. It has been shown that if the length scale is too small, the nonlocal FIP data is mesh dependent. But if the length scale is too large, the experimentally observed spread in fatigue life is not captured. This work introduces a nonlocal nonconformal volume (i.e., a volume that surrounds each element and overlaps nonlocal volumes). Averaging FIP over this nonlocal volume both captures the spread in fatigue data and is mesh independent. It also allows for weighted nonlocal averages that would have excluded some of the microstructure using the conformal approach. While this approach is more accurate than the previous approaches, it does require a large amount of computational resources to determine each nonlocal volume, so a parallelized algorithm that is scalable across multiple computing nodes is employed. The example polycrystalline material for this work is Ti-6Al-4V, a common titanium alloy with a hexagonal closed-packed crystal structure.

For alloys, larger inclusions, defects, or grains that are oriented to favor plasticity tend to lower the fatigue life of the material. However, when calculating a FIP at the microscale using computational crystal plasticity and finite element models, there is no intrinsic length scale associated with the model, and thus, FIPs do not automatically account for the size effect. Thus, McDowell et al³ introduced a length scale resulting in a nonlocal Fatemi-Socie FIP. Here, a crystallographic version of the Fatemi-Socie FIP is used and defined by

$$FIP^{(\alpha)} = \frac{\Delta \gamma_p^{(\alpha)}}{2} \left(1 + \kappa \frac{\sigma_n^{(\alpha)}}{\sigma_y} \right), \tag{1}$$

where $\Delta \gamma_p^{(\alpha)}$ is the range of plastic shear strains over a cycle and $\sigma_n^{(\alpha)}$ is the stress perpendicular to a slip plane, all for a slip system α ; σ_y is the yield strength. The constant κ accounts for load state. In the work here, only the maximum FIP value over all the slip systems (at a given material point) is stored. Here, κ is 0.55, and σ_y is 900 MPa (the average bulk yield strength given for Ti-6Al-4V in previous work⁵).

To account for the size dependence of fatigue life on microstructure size, the FIP value in Equation (1) is nonlocal. In the work here, every material point (i.e., integration point) is assigned a FIP, and these are averaged over a nonlocal region similar to the average volume of the crystallographic grains (as in Castelluccio and McDowell¹).

 $^{^{1}} Department\ of\ Mechanical\ Engineering,\ Marquette\ University,\ Milwaukee,\ Wisconsin,\ USA$

²Brookfield Academy, Brookfield, Wisconsin, USA

Yet the shape of this region and the approach to nonlocal averaging can take several forms. Castelluccio and McDowell¹ show that neglecting this nonlocal volume average-in a finite element simulation-results in a mesh dependent FIP value. They also consider averaging over crystallographic grains; this eliminates mesh dependence but reduces the spread in FIP values to an extent which no longer represents fatigue statistics observed experimentally. This approach also does not hold the nonlocal volume constant, so microstructures with a wide distribution of grain sizes could result in very high FIPs in a few small grains. Castelluccio and McDowell show that nonlocal volumes based on crystallographic slip planes result in both a realistic distribution of FIP and minimal mesh sensitivity. However, using as slip plane-based nonlocal volume requires predetermining the shape of a slip plane, which may become difficult for hexagonal closepacked (HCP) materials such as titanium where several slip planes carry significant shear stresses. In the study of Castelluccio and McDowell, they show that nonlocal volumes that contain more than one crystallographic grain have advantages; they state that their "results demonstrate the limitation of using an apparent Schmid factor (considering only grain orientation and ignoring intergranular interactions) as a predictor of fatigue crack formation."

Another disadvantage of nonlocal averaging over grains is that it does not address size effect; the model would produce the same result with large or small grains (unless a size-dependent constitutive law is implemented). Conversely, using a geometric nonlocal volume like a sphere or cube that is not based on the microstructure morphology allows the nonlocal volume to stay constant in size for large and small grains which in turn results in size effect.

Several studies use nonlocal volumes that contain more than one crystallographic grain; the studies^{1,2} predefine static nonlocal volumes for calculating FIP (i.e., they do not move in the microstructure). This approach requires that all nonlocal volumes be conforming, such that there is no space in the microstructure where FIP is not averaged. It also does not allow for overlapping volumes.

Enakoutsa et al⁶ pose a nonlocal ductile fracture model that addresses unlimited localization in porous solids—where the microstructural defects are pores. They propose an averaging method for porosity that is not uniform over a nonlocal volume and that "considerably improves numerical predictions." Reframing this approach in terms of FIP rather than porosity evolution rate gives

$$FIP^{\rm nl}(\boldsymbol{x}) = \frac{1}{A(\boldsymbol{x})} \int_{\Omega} \phi(\boldsymbol{x} - \boldsymbol{y}) FIP^{\rm loc}(\boldsymbol{y}) d\Omega, \qquad (2)$$

where FIP^{loc} and FIP^{nl} are local and nonlocal FIP values respectively. The position where nonlocal FIP is

calculated is \boldsymbol{x} and \boldsymbol{y} is positions around \boldsymbol{x} over which FIP^{loc} is integrated. The nonlocal volume is Ω , A is a normalizing value defined in Enakoutsa et al, 6 and

$$\phi(\mathbf{x}) = \exp(-||\mathbf{x}||^2/l^2),$$
 (3)

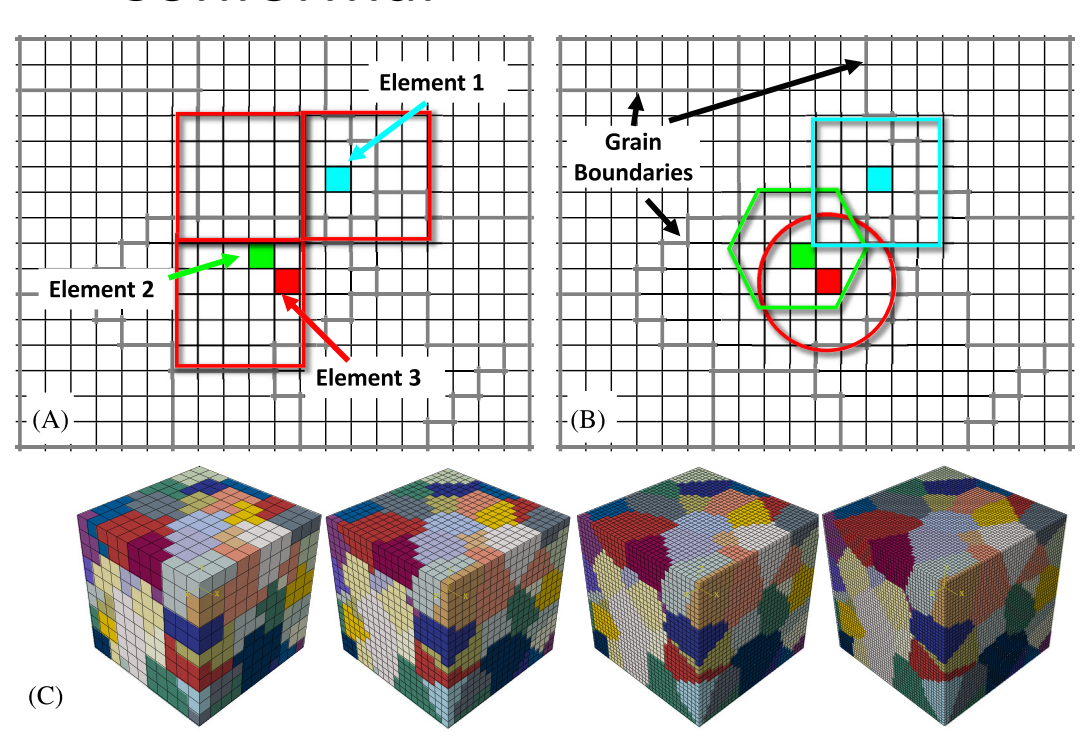
where l is the nonlocal length scale. For the work here, l is 13.37% of the length of the unit cell (which is based on achieving a nonlocal volume equal to the average grain volume). For nonlocal volumes that exceed the modeled domain, Ω is truncated. This truncation can also occur in conformal volumes.

If static conformal nonlocal volumes are used with the approach in Equation (2), then regions near the edge of each volume carry a much lower weight than regions near the volume's centroid. However, there is no reason that some regions of the microstructure should be excluded in this way when calculating nonlocal FIP. To remedy this issue, the work here uses dynamic nonlocal volumes (i.e., that move with the location at which FIP^{loc} is calculated) and are nonconformal (i.e., each volume can overlap with other volumes). This means that unique spherical volumes surround each point \boldsymbol{x} at which FIP^{loc} is calculated. So, every finite element has its own nonlocal volume. These conformal and nonconformal nonlocal volumes are shown in Figure 1.

While these dynamic nonconformal nonlocal volumes reduce mesh dependence while maintaining the statistical spread in FIP seen experimentally and account for FIPs across grain boundaries, they require the determination of a large number of nonlocal volumes. For example, if a microstructural mesh has 100,000 elements, then 100,000 nonlocal volumes are determined. For regular meshes, an algorithm can be formulated to efficiently determine these nonlocal volumes, but for irregular meshes, these nonlocal volumes need formulated by systematically searching the mesh. For that reason, an approach based on Python parallel processing is proposed here. This approach is scalable across many processors and computing nodes.

Determining each nonlocal volume is an *embarrassingly* parallel task, so it can scale (nearly) linearly across a large number of computing cores and computing nodes on a high-performance computing cluster. Since Python's multiprocessing module⁷ does not easily scale across several computing nodes, the work here uses the open-source Python library Dask⁸ for parallelization of pre-processing scripts (specifically the dask.distributed library) as shown in Moore et al.⁹

The crystal plasticity micromechanics model follows exactly the derivation of McGinty, ¹⁰ details of which are not reproduced here. The only modification comes from the slip kinetics,



(A) Static conformal nonlocal volumes (red boxes) around several finite elements in a polygranular microstructure. (B) Three nonconformal nonlocal volumes (colored shapes corresponding to the element colors); notice that the nonconformal volumes overlap, are centered around each element, and can be any shape. (C) 11³, 19³, 32³, and 48³ element meshes (left to right) where colors represent different grains. [Colour figure can be viewed at wileyonlinelibrary.com]

$$\dot{\gamma}^{(\alpha)} = \dot{\gamma}_0 \left| \frac{\tau^{(\alpha)} - a^{(\alpha)}}{\tau_0^{(\alpha)}} \right|^m \operatorname{sign}(\tau^{(\alpha)}), \tag{4}$$

where m is a material parameter, τ_0 is a reference shear stress, $\dot{\gamma}_0$ is a reference shear strain rate, $a^{(\alpha)}$ is a backstress that describes kinematic hardening, and $\tau^{(\alpha)}$ is the resolved shear stress. Unlike in McGinty, 10 the reference shear stress in each system is a weighting factor of a constant reference shear stress $\tau_0^{(\alpha)} = w\tau_0$ where w is a weighting factor and τ_0 is the constant reference shear stress. Four families of slip systems in the HCP α phase are considered: basal, prismatic, pyramidal $\langle a \rangle$, and pyramidal $\langle c + a \rangle$. The weighting factors w for the basal, prismatic, pyramidal $\langle \boldsymbol{a} \rangle$, and pyramidal $\langle \boldsymbol{c} + \boldsymbol{a} \rangle$ families are 1.0, 1.0, 1.13, and 2.12, respectively. The first three weights are used in Moore et al, 11 and the pyramidal $\langle c + a \rangle$ weight is determined to match the anisotropy of the material shown in Mulay et al. ¹² The $\langle c \rangle$ to $\langle a \rangle$ ratio is 1.599. Only the α phase is modeled; this approximation should result in minimal error in stress-strain response as discussed in Moore et al. 11

The finite element model uses four different meshes ranging from coarse to fine that match exactly the mesh

sizes used in Castelluccio and McDowell. These meshes 48 elements, respectively. Abaqus (2018) software with reduced integration* hexahedral eight node finite elements are used exclusively. A displacement is applied in the x-direction; subsequently, the displacement in the yand z-directions change based on the apparent Poisson's ratio of the material. Each microstructure mesh is loaded cyclically for three full cycles and a strain amplitude of 0.5% and an R ratio of -1. This amounts to a max/min average stress of \pm 600 MPa.

Fifty different realizations of microstructures are used for each mesh. Each realization has 100 randomly distributed equiaxed crystallographic grains with a constant Euler angle for each grain. The crystallographic texture is random. The grain morphology for each microstructure realization is created using tessellation in the software Neper. 13 The elastic parameters in Voigt notation are $C_{11} = 162,400 \text{ MPa}, C_{12} = 92,000 \text{ MPa}, C_{44} = 69,000 \text{ MPa}.$ The plasticity material parameters are $\dot{\gamma}_0 = 0.001 \, \text{s}^{-1}$,

^{*}Post-processing software is written to find the maximum FIP over several integration points were standard integration elements to be used.

.4602695, 0, Downloaded from https://onlinelibrary.wiley.com/doi/10.1111/ffe.14158 by Lawrence

Livermore National Laboratory, Wiley Online Library on [14/10/2023]. See the Terms and Conditions (https://onlinelibrary.wiley

litions) on Wiley Online Library for rules of use; OA articles are governed by the applicable Creative Commons Licens

FIGURE 2 Equivalent stress and fatigue life for a Ti-6Al-4V plate cycled at various R ratios: -1 (\spadesuit), -0.4 (\blacktriangle), 0 (+), 0.1 (\times), and 0.3 (\spadesuit). The simulated FIP values (in a given fitting stress range) are converted to fatigue life via fitting parameters. [Colour figure can be viewed at wileyonlinelibrary.com]

m = 50, $\tau_0 = 334$ MPa, and the direct hardening parameter (h in McGinty¹⁰) is 500 MPa; all other hardening parameters in McGinty¹⁰ are zero. These parameters are calibrated to data from Mulay et al. ¹² Before presenting the statistical spread predictions from the model, the spread observed in Ti-6Al-4V fatigue data is addressed. Since fatigue life is measured experimentally while FIP is calculated by the model, each measured fatigue life is converted to FIP. To do this, FIP values from all four meshes and nonlocal volume average procedures are fit to life data.

For this fitting, a single realization of the microstructure from Figure 4 is simulated for a maximum stress of 586, 600, and 655 MPa and R=-1. This realization is chosen to give FIP values in the middle of each of the lowest histogram bin in Figure 4 and is considered to represent the expected FIP value. The simulated FIPs are fit to the best fit equivalent stress line for the fatigue life of a solution treated and aged Ti-6-Al-4V plate (from the MMPDS handbook) in Figure 2. In Figure 2, the difference between the fit fatigue life values for each mesh size and nonlocal volume is negligible even though each set of fitting parameters (mapping FIP to N) is different. Using $FIP = AN^b$, the fitting parameters are A and b; these are used to convert the histogram of fatigue life from Figure 2 to FIP values.

The probability density function for FIP values converted from fatigue life using the fitting parameters discussed above are shown in Figure 3. Each fatigue life in

the fitting range shown in Figure 2 is converted to FIP to give an estimate of the experimentally observed statistical spread in FIP values. For each case, a three parameter Weibull distribution is fit to the probability density function using Python's scipy.stats.exponweib function. These Weibull distributions are compared to simulations in Figure 4.

Figure 4 shows FIP results using four types of nonlocal volume averages for each of the four mesh sizes (i.e., $11 \times 11 \times 11$, $19 \times 19 \times 19$, $32 \times 32 \times 32$, and $48 \times 48 \times 48$ elements). The local FIP values for each mesh size are the same, but the averaging volume and the averaging procedure differ.

FIP values denoted as *element* are not averaged (i.e., the nonlocal volume is only one element). The FIP values denoted as *conformal* use cubic nonlocal volumes that do not overlap (as shown in Figure 1A). The FIP values denoted as *nonconformal* use spherical overlapping nonlocal volumes centered at every element (as shown in Figure 1B); for the *nonconformal* average, every FIP is weighted equally. The FIP values denoted as *weighted* use the same nonlocal volumes as the *nonconformal* average but weight each element's FIP values using Equation (2).

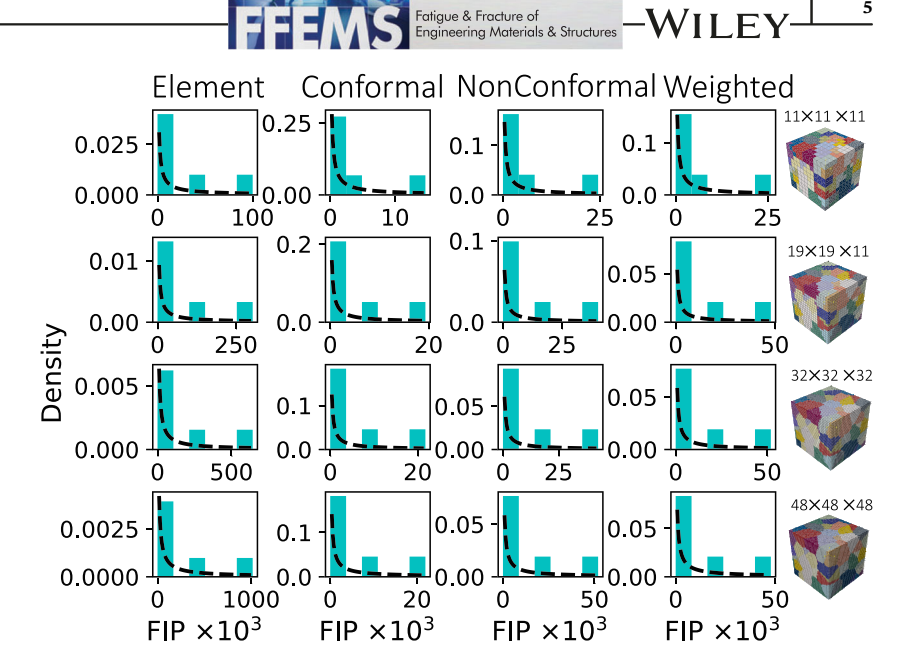
The error shown in Figure 4 is calculated using

$$e = 100\% \frac{\max(FIP_{\text{model}}^{\text{nl}}) - \max(FIP_{\text{exp.}}^{\text{nl}})}{\max(FIP_{\text{exp.}}^{\text{nl}})}.$$
 (5)

As shown in Figure 4, the local *element* value of FIP has a large spread but also a large mesh dependence. For the conformal nonlocal volumes, the mesh dependence is

[†]Equivalent stress as defined by MMPDS is stress "that consolidates data for all stress ratios into a single curve"; it is not the von Mises stress.

FIGURE 3 The probability density function (i.e., density) for each mesh size and nonlocal volume is shown (by the dashed line) based on the fatigue life in the fitting range in Figure 2. The density is determined from the normalized histograms. [Colour figure can be viewed at wileyonlinelibrary.com



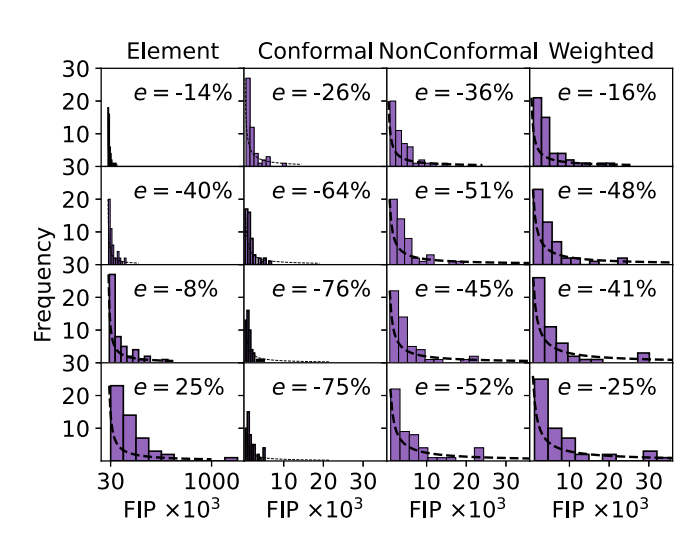


FIGURE 4 FIP for 50 realizations, using a local element volume, a conformal nonlocal volume, a nonconformal nonlocal volume, and a weighted nonconformal nonlocal volume. The coarse to fine meshes are top to bottom, respectively. The probability density functions from Figure 3 are scaled to the maximum histogram value and shown with dashed lines. The error e is also given as a percentage (where negative values indicate that the simulation underestimates the data). [Colour figure can be viewed at wileyonlinelibrary.com]

minimal, but the spread is limited. For the nonconformal volumes, the mesh dependence is also minimal, but the spread is wider than the conformal volume, albeit not as wide as the element local FIP.

The $48 \times 48 \times 48$ element mesh with the element nonlocal volume average is the only to over-predict the data. All other predictions under-predict the data. For the $32 \times$ 32×32 and $48 \times 48 \times 48$ elements meshes, the effect of nonconformal nonlocal volumes is the most clear. While

the mesh dependent element averages for the $32 \times 32 \times$ 32 and $48 \times 48 \times 48$ element meshes show -8% and 25% error, respectively, the mesh independent conformal element averages show -76% and -75%, respectively. This error is reduced for the mesh independent nonconformal element averages, where for the $32 \times 32 \times 32$ and $48 \times$ 48×48 element meshes, the error ranged from -16% to -52%. The weighted average shows between 3% and 27% less error than for the nonconformal average; thus, the weighted nonconformal average is considered more accurate than the nonconformal average without weighting.

This letter's intent is to convey that a weighted nonconformal nonlocal average is computationally tractable and has potential to predict a more accurate statistical spread in FIP values than other mesh independent nonlocal approaches considered.

ACKNOWLEDGMENTS

This work was supported by the National Science Foundation, Division of Civil, Mechanical and Manufacturing Innovation's (CMMI) Mechanics of Materials and Structures (MOMS) program under Grant No. Award Number 1934753. The author's would like to thank Dr. Dinc Erdeniz of U. Cincinnati for his discussion about and support of this work.

DATA AVAILABILITY STATEMENT

The data that support the findings of this study are available from the corresponding author upon reasonable request.

ORCID

John A. Moore https://orcid.org/0000-0001-5496-7004



REFERENCES

- Castelluccio GM, McDowell DL. Microstructure and mesh sensitivities of mesoscale surrogate driving force measures for transgranular fatigue cracks in polycrystals. *Mater Sci Eng A*. 2015;639:626-639.
- 2. Castelluccio GM, McDowell DL. Assessment of small fatigue crack growth driving forces in single crystals with and without slip bands. *Int J Fract.* 2012;176(1):49-64.
- Kumar R, Wang AJ, McDowell D. Effects of microstructure variability on intrinsic fatigue resistance of nickel-base superalloys—a computational micromechanics approach. *Int J Fract*. 2006;137(1-4):173-210.
- 4. Fatemi A, Socie DF. A critical plane approach to multiaxial fatigue damage including out-of-phase loading. *Fatigue Fract Eng M.* 1988;11(3):149-165.
- 5. United States, and Battelle Memorial Institute. *MMPDS-01 Metallic Materials Properties Development and Standardization (MMPDS)*: Federal Aviation Administration; 2008.
- Enakoutsa K, Leblond J, Perrin G. Numerical implementation and assessment of a phenomenological nonlocal model of ductile rupture. *Comput Methods Appl Mech Numerical Eng.* 2007; 196(13-16):1946-1957.
- 7. Multiprocessing—process-based parallelism. https://docs.python.org/3/library/multiprocessing.html
- 8. Dask Development Team. Dask: Library for Dynamic Task Scheduling: Dask; 2016. https://dask.org

- 9. Moore JA, Martinez C, Chandel A. NonlOCAL Results Processor for Finite Element Analysis (NOCAL-FEA). *Softw Impacts*. 2023. submitted. https://doi.org/10.5281/zenodo.8323192
- 10. McGinty R. *Multiscale Representation of Polycrystalline Inelasticity*: Georgia Institute of Technology; 2001.
- 11. Moore JA, Barton NR, Florando J, Mulay R, Kumar M. Crystal plasticity modeling of β phase deformation in Ti-6Al-4V. *Modell Simul Mater Sci Eng.* 2017;25(7):75007.
- 12. Mulay R, Moore J, Florando J, Barton N, Kumar M. Microstructure and mechanical properties of Ti-6Al-4V: mill-annealed versus direct metal laser melted alloys. *Mater Sci Eng A*. 2016;666:43-47.
- Quey R, Dawson P, Barbe F. Large-scale 3D random polycrystals for the finite element method: generation, meshing and remeshing. Comput Methods Appl Mech Eng. 2011;200(17-20): 1729-1745.

How to cite this article: Moore JA, Martinez C, Chandel A. A nonconformal nonlocal approach to calculating statistical spread in fatigue indicator parameters for polycrystals. *Fatigue Fract Eng Mater Struct.* 2023;1-6. doi:10.1111/ffe.14158